Effects of CO/CO2/NO on elemental lead adsorption on carbonaceous surfaces

2 authors, including:

Weijie Yang
North China Electric Power University
60 PUBLICATIONS **855** CITATIONS

SEE PROFILE

Some of the authors of this publication are also working on these related projects:

Project Study on structure-property relationships in single atom catalysts View project

CrossMark

ORIGINAL PAPER

Effects of CO/CO₂/NO on elemental lead adsorption on carbonaceous surfaces

Zhengyang Gao[1] · Weijie Yang[1]

Abstract The adsorption processes of elemental lead on carbonaceous surfaces which adsorbed $CO/CO_2/NO$ flue gases were investigated to understand the effects of $CO/CO_2/NO$ on elemental lead adsorption on carbonaceous surfaces with density functional theory. All calculations including optimizations, energies, and frequencies were conducted at B3PW91 density functional theory level, utilizing SDD basis set for lead and 6-31G(d) Pople basis set for other atoms. The results indicate that CO, CO_2, and NO can promote the adsorption of elemental lead on the carbonaceous surface, but probably compete for adsorption sites with elemental lead. The promotion effects on adsorption can be attributed to active sites on the carbonaceous surface rather than flue gas adsorption on the carbonaceous surface. In addition, the adsorption order of three kinds of flue gas on the carbonaceous surface is $CO_2 > NO > CO > Pb$ on average. Furthermore, the enhancement order of three kinds of flue gas on the elemental lead adsorption on carbonaceous surfaces is CO-CS > CO_2-CS > NO-CS > CS in general. In particular, atomic charge and adsorption energy have good linear relationship in the process of elemental lead adsorption.

Keywords Adsorption · Carbonaceous surface · DFT · Elemental lead

Introduction

Lead (Pb) pollution is recognized as a global concern due to its potential of causing irreversible damage in multiple respects. In organisms, lead is considered as unsafe at any concentration level [1]. Since lead is bio-accumulative it may be delivered to the human body through the food chain, thus becoming a major pollution agent [2]. In addition, lead pollution exerts a negative impact on the intelligence of children, hindering their ability to learn [3, 4]. For these reasons, prevention and control of lead pollution are issues of major importance.

Its contamination in the environment derives from natural and anthropogenic factors. The main pollution sources result from human activities such as coal combustion, mining activities, Pb containing paints, leaded gasoline and insecticides [5]. As lead was added to the gasoline as antiknock additives, leaded gasoline was considered to be the main source of lead pollution [6]. Once the relationship between leaded gasoline and lead pollution was realized, the atmospheric lead concentrations began to decrease for the first time owing to the phase-out of leaded gasoline [7]. Although leaded gasoline was forbidden, the lead concentration in the atmosphere remained at a high level. For example, the average Pb concentration is 224 ng/m3 in Shanghai [8, 9]. Coal pollution survey results showed that the average annual growth rate of lead emissions from coal was 9.55 % and the lead emissions of coal exceeded 14,000 t which was 35 times the amount of lead emissions of automobile exhaust by 2010 [10]. Apart from these, there was a significant positive correlation between the amount of coal combustion and the rate of lead poisoning in children [11]. Therefore, the main source of atmosphere lead pollution is the lead in coal combustion.

Lead in coal is released into the flue gas in the process of coal combustion, and the lead undergoes a series of physical and chemical changes along with temperature decreasing. Lead in the flue gas is commonly classified into two forms

✉ Weijie Yang
   18331121421@163.com

1 School of Energy and Power Engineering, North China Electric
   Power University, Baoding 071003, China

according to the different styles: gas lead (Pb$_g$) including elemental lead (Pb^0) and oxidation lead (Pb^{2+}) and particulate bound lead (Pb$_p$) [11]. In contrast to Pb^0, Pb^{2+} can be easily removed by wet flue gas desulfurization (WFGD) due to its property of water-soluble. As a consequence of the adsorption of fly ash, Pb^0 and Pb^{2+} can be transformed into particulate bound lead. In the light of the trapping effect of dust removal equipment of power station on the fly ash, the Pb$_p$ also can be effectively removed [12]. In conclusion, adsorption and oxidation of elemental lead is the effective method for controlling lead emissions.

In practical operation, there was no single and effective control method for Pb removal, but together with the removal of trace elements such as Hg. Carbonaceous adsorbent injection method is the most effective measure for removal of mercury, and a tremendous quantity of theoretical and experimental research works related to mercury adsorption on carbonaceous surfaces have been conducted [13–19]. However, there has been little research on lead adsorption on carbonaceous surfaces. Furthermore, the research related to the effect of flue gases on the adsorption of elemental lead on carbonaceous surfaces is particularly rare.

According to the present research situation, this paper attempts to investigate the mechanism of elemental lead adsorption on carbonaceous surfaces as well as the effects of different flue gases on the process of elemental lead adsorption on carbonaceous by quantum chemistry.

## Methods

Choice of model carbon

In the research of quantum chemistry, the structure of single layer graphite was usually used to simulate the structure of carbonaceous surfaces (CS) [20–25]. Chens et al. determined the seven rings zigzag benzene clusters (C$_{25}$H$_9$) structure for the surface structure of carbonaceous molecular simulation by comparing six different benzene ring structures [26]. Liu et al. successfully investigated the effects of chemical functional groups on mercury adsorption on carbonaceous surfaces by utilizing the five rings zigzag benzene cluster structure (C$_{19}$H$_8$) [27]. Considering the influence of accuracy and time, the five rings zigzag benzene cluster structure was applied to simulate the model of carbonaceous surfaces in this paper. Moreover, three unsaturated carbon atoms were applied to represent the active sites, and the other carbon atoms were closed by H atoms. The optimized geometry of the carbonaceous model is shown in Fig. 1.

Choice of method

In recent years, the density functional theory (DFT) has been widely applied to the calculation of quantum chemistry due to its well calculation accuracy and excellent calculation speed. B3PW91 together with the 6-31G(d) basis set has been validated to be accurate in calculating the adsorption on the carbonaceous surface [28, 29]. According to the large amount of electrons in heavy elements, effective core potential (ECP) was employed to replace the inner electrons of lead in order to save the computational cost. Therefore, Stuttgart group basis set (SDD) was utilized to take into account the relativistic effects [28]. In the light of the spin multiplicity effect, the lowest energy structure was selected for the ground state structure through energy calculation with different spin multiplicities [28]. In this work, all of the calculations including geometry optimizations, vibrational frequency analysis, and energy calculation were carried out at the B3PW91/SDD level for Pb atom and the B3PW91/6-31g(d) for other atoms in their electronic ground state.
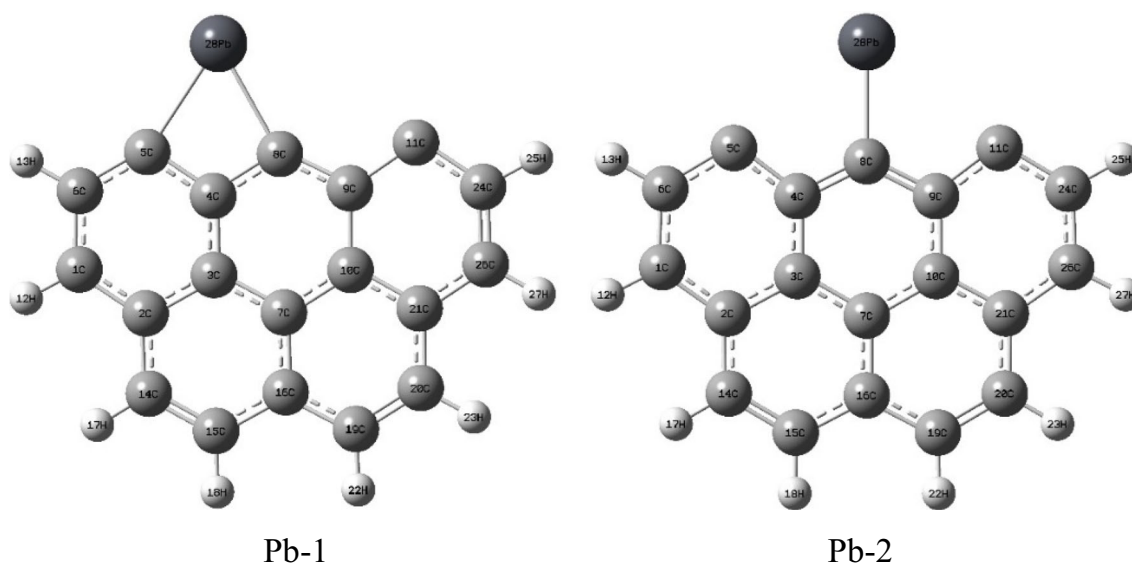
Fig. 1 Carbonaceous surface model

Pb-1

Pb-2
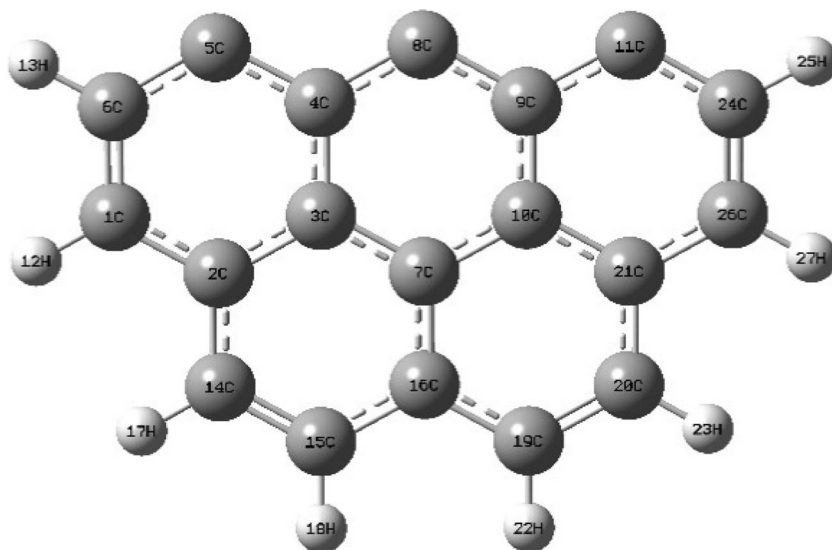
Fig. 2 Pb adsorption on carbonaceous surface models

The Gaussian09 software package was used for the density functional theory calculations of CO, CO$_2$, NO, and elemental lead adsorption on carbonaceous surfaces in this work [30]. The geometric models of carbonaceous surfaces and their corresponding Pb-CS, CO-CS, CO$_2$-CS, and NO-CS intermediates were fully optimized in their electronic ground state. Moreover, frequency calculations were performed so as to confirm their stability. The zero-point energy (ZPE) and single point energy were obtained to complete the energy calculation.

The adsorption energy (E$_{ads}$) was obtained by calculating total energy of the whole adsorption system and total energy of the separate reactants before combination. As presented in following equation:

$$E_{ads} = E_{AB} - (E_A + E_B) \qquad (1)$$

where E$_A$ is the total energy of the adsorbate, and E$_B$ is the total energy of the substrate, while E$_{AB}$ is the total energy of adsorbate/substrate system in equilibrium state. A higher negative value of E$_{ads}$ presents a stronger adsorption. If the value of E$_{ads}$ is at the range of −10 ~ −30 kJ mol^{-1}, the adsorption belongs to physical adsorption. If the value of E$_{ads}$ is at the range of −50 ~ −960 kJ mol^{-1}, the adsorption belongs to chemical adsorption [31].

Furthermore, the adsorption of elemental lead on the carbonaceous surface was investigated by calculating the bond length, bond population, Mulliken charge, and adsorption energy. The bond strength can be presented roughly by the Mulliken bond population. The charge of Pb atom can be obtained by calculating the Mulliken charge.

Results and discussion

Pb adsorption on the carbonaceous surface

In order to research the effect of different flue gas components on elemental lead adsorption on carbonaceous surfaces, the adsorption characteristics of lead on carbonaceous surfaces should be investigated first. There were two kinds of models for which elemental lead was adsorbed on the carbonaceous surface in Fig. 2. C-Pb bond lengths, bond population, Pb charge, and E$_{ads}$ were calculated, as presented in Table 1.

Comparing the two different adsorption models, despite the C-Pb bond length of Pb-CS-2 model is shorter than Pb-CS-1 model and the Pb charge of Pb-CS-2 model is larger than Pb-CS-1 model, Pb-CS-1 model which contains double bonds has a larger adsorption energy.

Pb adsorption on CO-CS surface

There were four kinds of carbon monoxide adsorption models on the carbonaceous surfaces, which can be seen from Fig. 3.

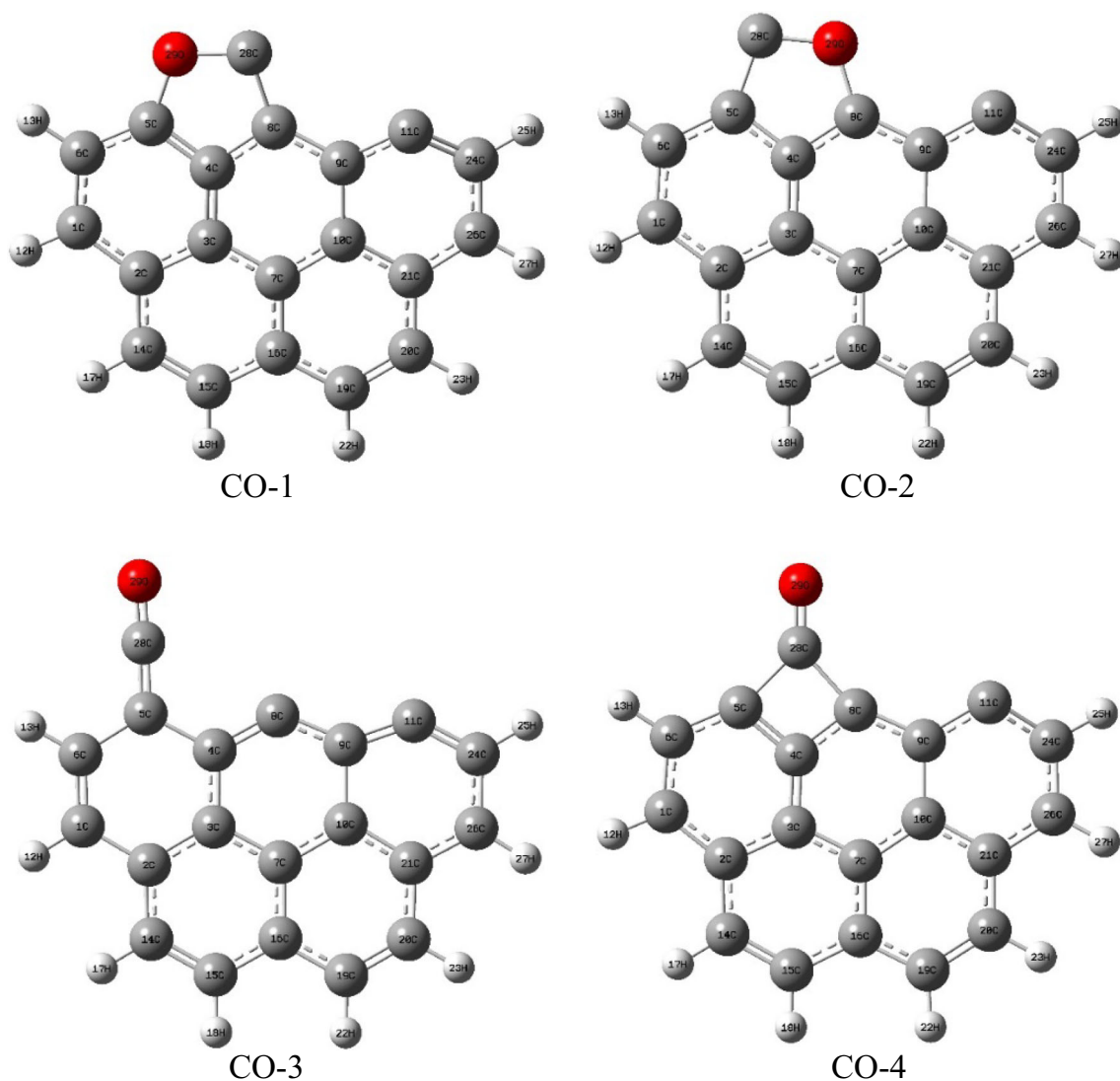| Table 1 Pb adsorption on carbonaceous surface parameters	Model	Bond	Bond lengths(Å)	Bond population	Pb charge	E$_{ads}$(kJ mol^{-1})
	Pb-CS-1	C(5)- Pb(28)	2.335	0.220883	0.580928	−186.8
		C(8)-Pb (28)	2.250	0.239911		
	Pb-CS-2	C(8)-Pb(28)	2.130	0.286439	0.510179	−103.1

Fig. 3 CO adsorption on carbonaceous surface models

Bond lengths, bond population, and E_{ads} were achieved, as reported in Table 2. The parameters in Table 2 confirmed that CO adsorption on the carbonaceous surface belongs to chemical adsorption due to E_{ads} at the range of $-50 \sim -960$ kJ mol^{-1}. Comparing the difference of adsorption energy between Tables 1 and 2, the adsorption of CO on the carbonaceous

Table 2 CO adsorption on carbonaceous surface parameters

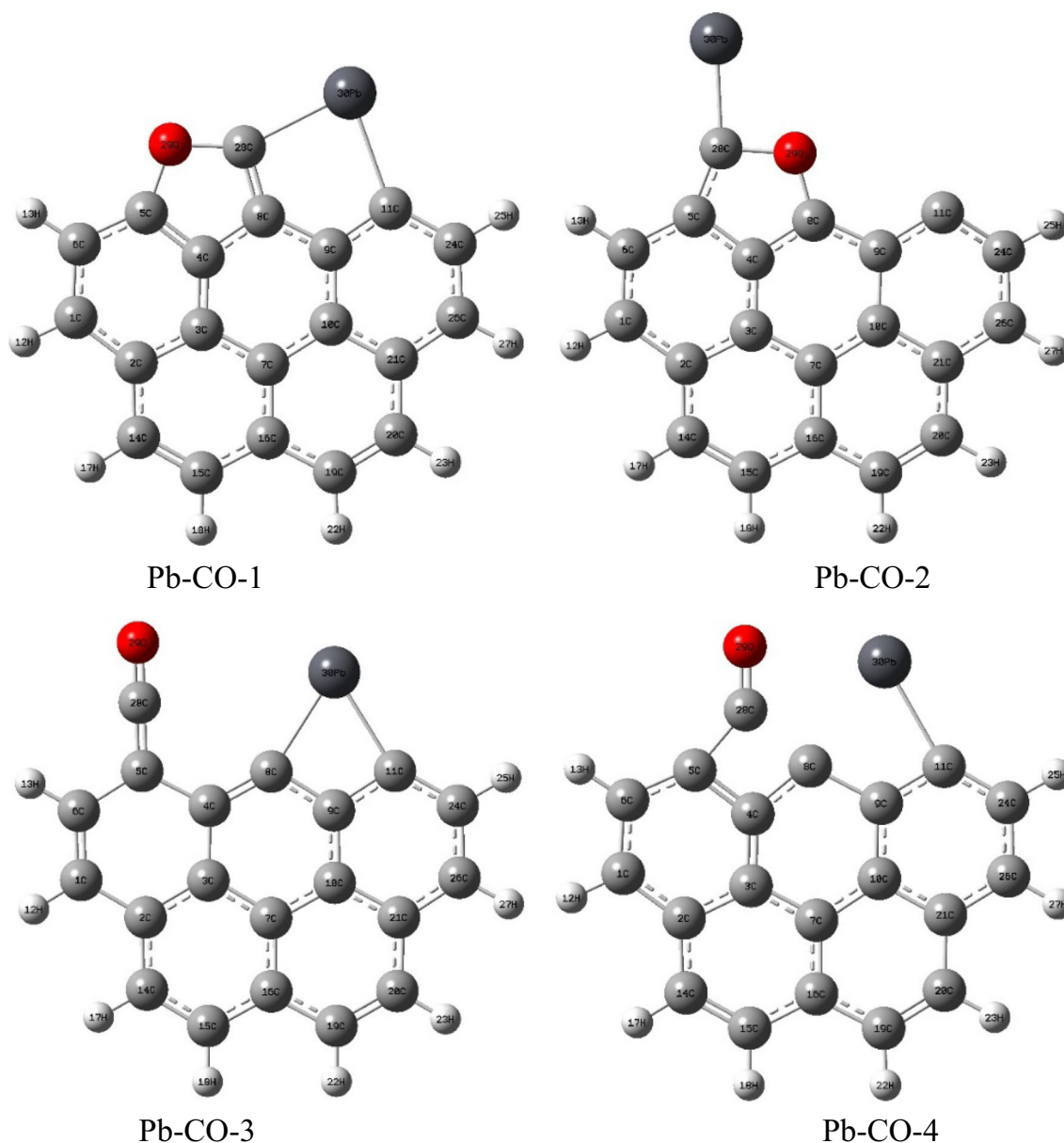| Model	Bond	Bond lengths(Å)	Bond population	E_{ads}(kJ mol^{-1})
CO-CS-1	C(5)-O(29)	1.408	0.170989	−227.5
	O(29)-C(28)	1.379	0.241879	
	C(28)-C(8)	1.478	0.429591	
CO-CS-2	C(5)-C(28)	1.488	0.382789	−227.9
	C(28)-O(29)	1.384	0.242527	
	O(29)-C(8)	1.396	0.196805	
CO-CS-3	C(5)-C(28)	1.339	0.392278	−254.8
	C(28)-O(29)	1.166	0.591313	
CO-CS-4	C(5)-C(28)	1.584	0.186182	−303.3
	C(28)-O(29)	1.192	0.561962	
	C(28)-C(8)	1.584	0.184383	

Pb-CO-1

Pb-CO-2

Pb-CO-3

Pb-CO-4

Fig. 4 Pb adsorption on CO-CS models

surface is much firmer than elemental lead on carbonaceous surface, revealing that there may be a competitive adsorption between CO and elemental lead.

The lead atom was placed in the vicinity of different active sites for geometry optimization, and four different adsorption models were obtained, as shown in Fig. 4. Bond lengths, bond population, Pb charge, and E_{ads} were achieved, as presented in Table 3.

Comparing the difference of adsorption energy between Tables 1 and 3, the absolute value of the E_{ads} becomes larger,

Table 3 Pb adsorption on CO-CS parameters

Model	Bond	Bond lengths(Å)	Bond population	Pb charge	E_{ads}(kJ mol^{-1})
Pb-CO-CS-1	C(28)-Pb(30)	2.273	0.267094	0.530955	−626.9
	C(11)-Pb(30)	2.339	0.244886		
Pb-CO-CS-2	C(28)-Pb(30)	2.136	0.36948	0.432043	−138.2
Pb-CO-CS-3	C(11)-Pb(30)	2.258	0.260041	0.491118	−546.1
	C(8)-Pb(30)	2.289	0.229282		
Pb-CO-CS-4	C(11)-Pb(30)	2.299	0.208171	0.451707	−324.0

CO$_2$-1   CO$_2$-2
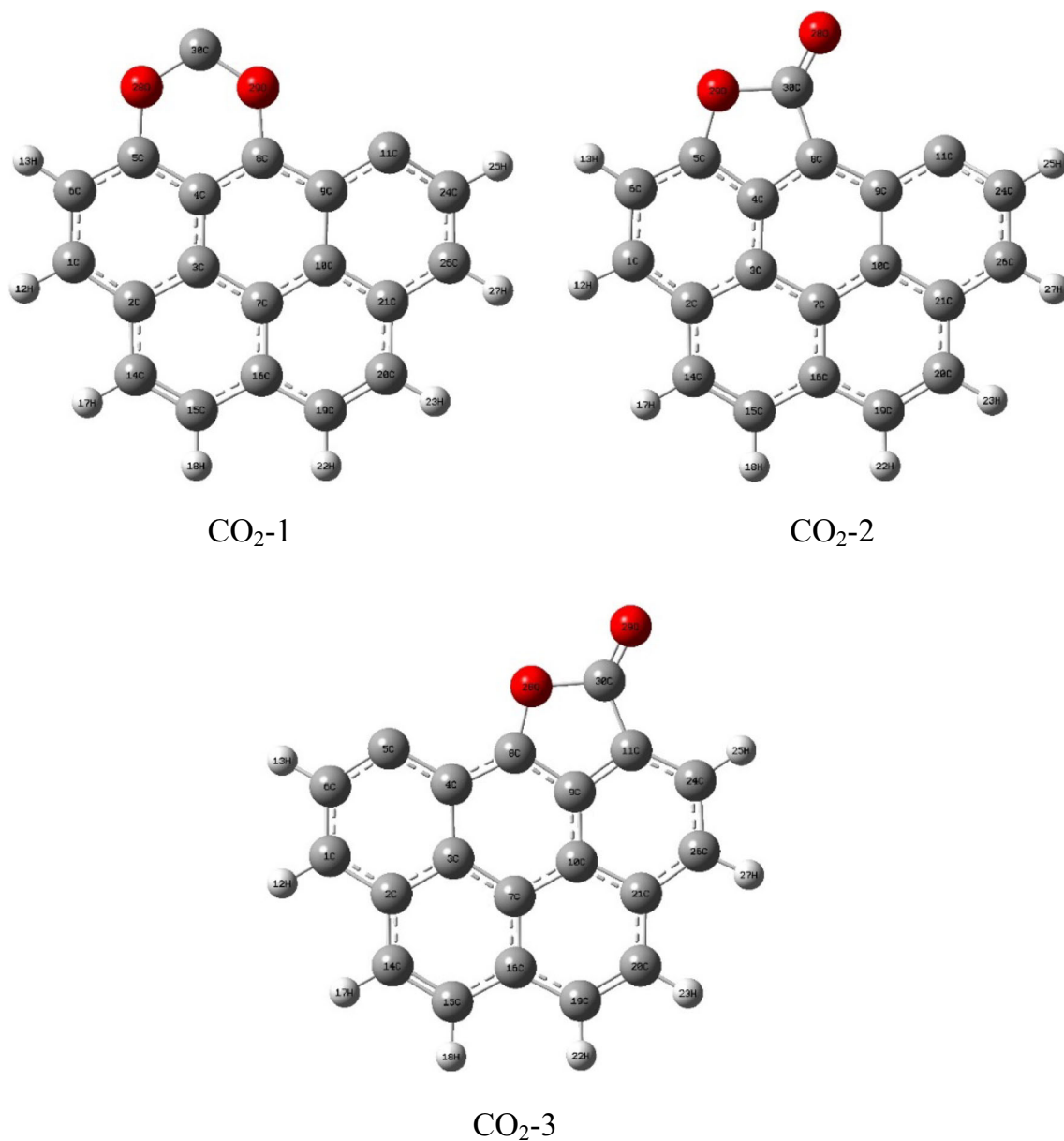

CO$_2$-3

Fig. 5 CO$_2$ adsorption on carbonaceous surface models

Table 4 CO$_2$ adsorption on carbonaceous surface parameters

Model	Bond	Bond lengths(Å)	Bond population	E$_{ads}$(kJ mol^{-1})
CO$_2$-CS-1	C(5)-O(28)	1.384	0.18387	−179.1
	O(28)-C(30)	1.354	0.181145	
	C(30)-O(29)	1.346	0.204384	
	O(29)-C(8)	1.382	0.21979	
CO$_2$-CS-2	C(5)-O(29)	1.367	0.240799	−392.2
	O(29)-C(30)	1.453	0.233616	
	C(30)-O(28)	1.196	0.593024	
	C(30)-C(8)	1.485	0.236558	
CO$_2$-CS-3	C(8)-O(28)	1.358	0.270897	−405.1
	O(28)-C(30)	1.450	0.217027	
	C(30)-O(29)	1.196	0.617073	
	C(30)-C(11)	1.482	0.206123	

indicating that the addition of CO molecule enhances the process of Pb adsorption on carbonaceous surface. In addition, the bond population also became larger at different degrees, confirming the CO enhancement effect on elemental lead adsorption. In particular, the adsorption energy of Pb-CO-CS-2 model is minimal among the four different models, because the Pb atom is not adsorbed on the active site of carbonaceous surface but on the carbon atom of CO molecule. According to this phenomenon, it would seem logical to assume that the elemental lead is more likely to adsorb on the active site of

carbonaceous surface than CO molecule which adsorbed on the carbonaceous surface.

Pb adsorption on CO_2-CS surface

There were three kinds of carbon dioxide adsorption models on carbonaceous surfaces, as shown in Fig. 5. Bond lengths, bond population, and E_{ads} were obtained, as presented in Table 4. From Table 4, the adsorption energy of CO_2 on the carbonaceous surface belongs to chemical adsorption.
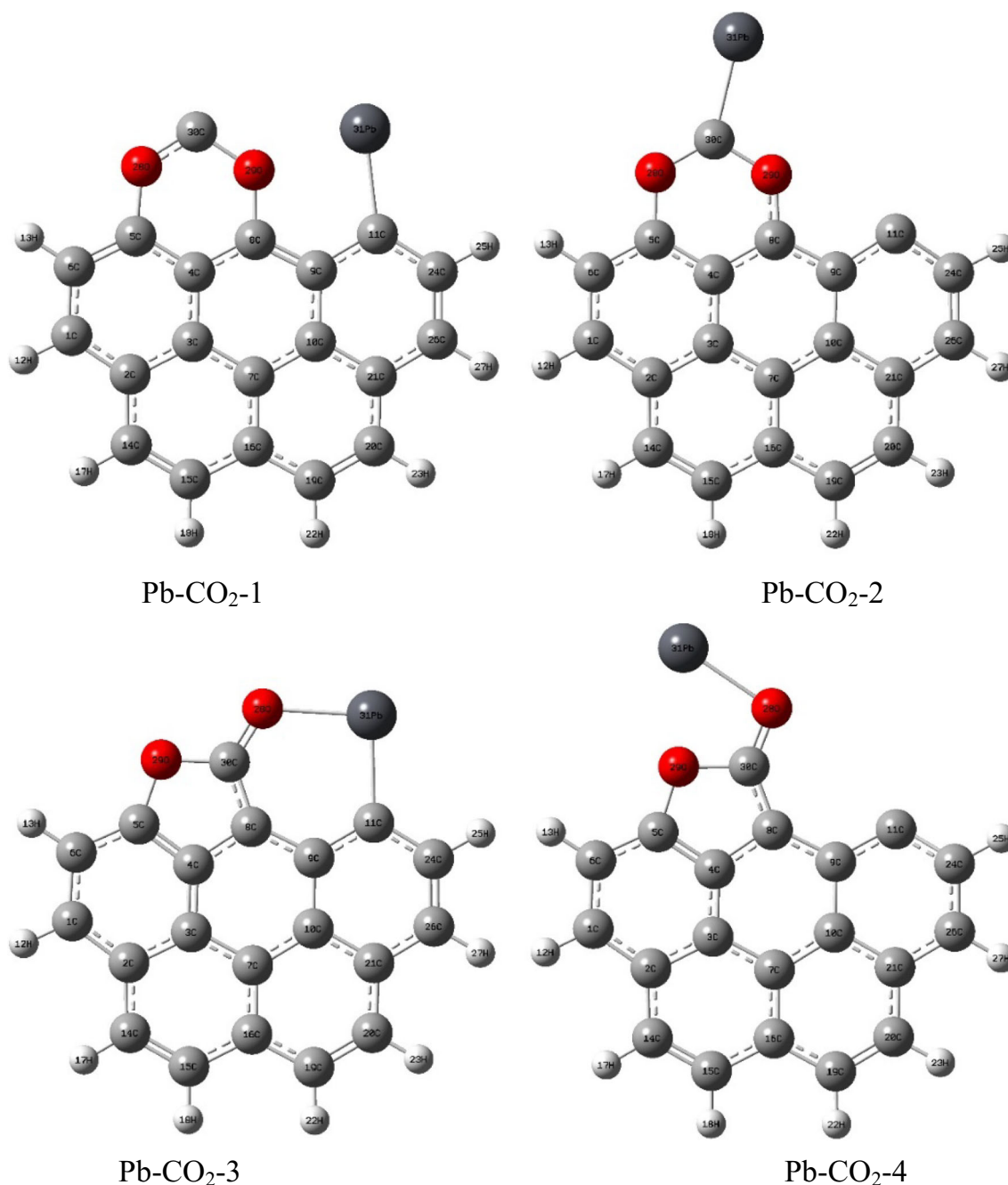

Pb-CO$_2$-1

Pb-CO$_2$-2

Pb-CO$_2$-3

Pb-CO$_2$-4

Fig. 6 Pb adsorption on CO_2-CS models

Table 5 Pb adsorption on CO_2-CS parameters

Model	Bond	Bond lengths(Å)	Bond population	Pb charge	E_{ads}(kJ mol^{-1})
Pb-CO_2-CS-1	C(11)-Pb(31)	2.157	0.375189	0.398164	−425.8
Pb-CO_2-CS-2	C(30)-Pb(31)	2.154	0.361905	0.234999	−171.4
Pb-CO_2-CS-3	C(11)-Pb(31)	2.202	0.330725	0.598364	−542.6
	O(28)-Pb(31)	2.217	0.134266		
Pb-CO_2-CS-4	O(28)-Pb(31)	2.285	0.149135	0.139947	−151.8

Comparing the difference of adsorption energy between Tables 1 and 4, the adsorption of CO_2 on the carbonaceous surface is much more stable than elemental lead on the carbonaceous surface, suggesting that there could be a competitive adsorption between CO_2 and Pb.

The lead atom was placed in the vicinity of different active sites for geometry optimization, and four different adsorption models were obtained, as shown in Fig. 6. Bond lengths, bond population, Pb charge, and E_{ads} were achieved, as presented in Table 5.

Comparing the difference in adsorption energy between Tables 1 and 5, the absolute value of the E_{ads} becomes larger, indicating that the addition of CO_2 molecule enhances the process of Pb adsorption on carbonaceous surfaces. Consistent with Pb adsorption on CO-AC surface, the elemental lead is more likely to adsorb on the active site of the carbonaceous surface than the CO_2 molecule which adsorbed on the carbonaceous surface according to the value of adsorption energy in Table 5 and adsorption models in Fig. 6.

Pb adsorption on NO-CS surface

As Fig. 7 demonstrates, there were two kinds of nitric oxide adsorption models on the carbonaceous surface. Bond lengths, bond population, and E_{ads} were obtained, as presented in
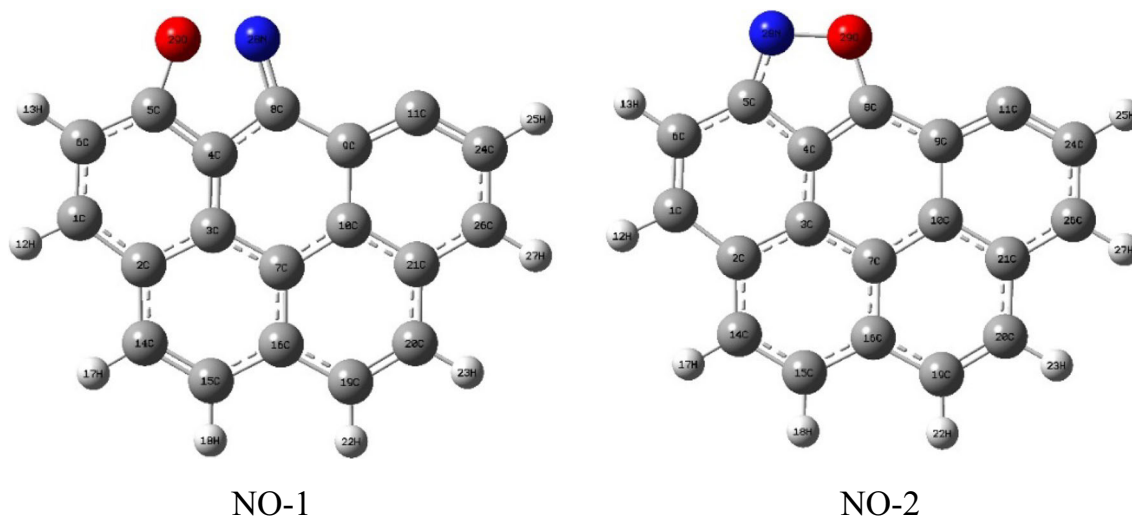
Table 6. From Table 6, NO adsorption on the carbonaceous surface belongs to chemical adsorption, owing to the E_{ads} at the range of −50 ∼ −960 kJ mol^{-1}. Comparing the difference of adsorption energy between Tables 1 and 6, the adsorption of NO on the carbonaceous surface is much firmer than elemental lead on the carbonaceous surface, suggesting that there may be a competitive adsorption between NO and Pb.

The lead atom was placed in the vicinity of different active sites for geometry optimization, and four different adsorption models were obtained, as shown in Fig. 8. Bond lengths, bond population, Pb charge, and E_{ads} were achieved, as presented in Table 7. It is obvious that the adsorption of elemental lead on the carbonaceous surface which adsorbed NO molecule belongs to chemical adsorption.

Comparing the difference of adsorption energy between Tables 1 and 7, the absolute value of the E_{ads} becomes larger which indicates that the addition of NO molecule promotes the process of elemental lead adsorption on the carbonaceous surface. From Table 7 and Fig. 8, the adsorption energy of Pb-NO-CS-2 and Pb-NO-CS-4 models are smaller than the other two models, confirming that the elemental lead is more likely to adsorb on the active site of the carbonaceous surface than the NO molecule which adsorbed on the carbonaceous surface.

NO-1   NO-2

Fig. 7 NO adsorption on carbonaceous surface models

Model	Bond	Bond lengths(Å)	Bond population	E_ads(kJ mol⁻¹)
NO-CS-1	C(5)-O(29)	1.358	−0.000465	−304.4
	O(29)-N(28)	1.442	0.002205	
	N(28)-C(8)	1.322	−0.001989	
NO-CS-2	C(5)-N(28)	1.330	0.000723	−336.5
	O(29)-N(28)	1.439	0.002897	
	O(29)-C(8)	1.350	−0.004099	

Table 6 NO adsorption on carbonaceous surface parameters
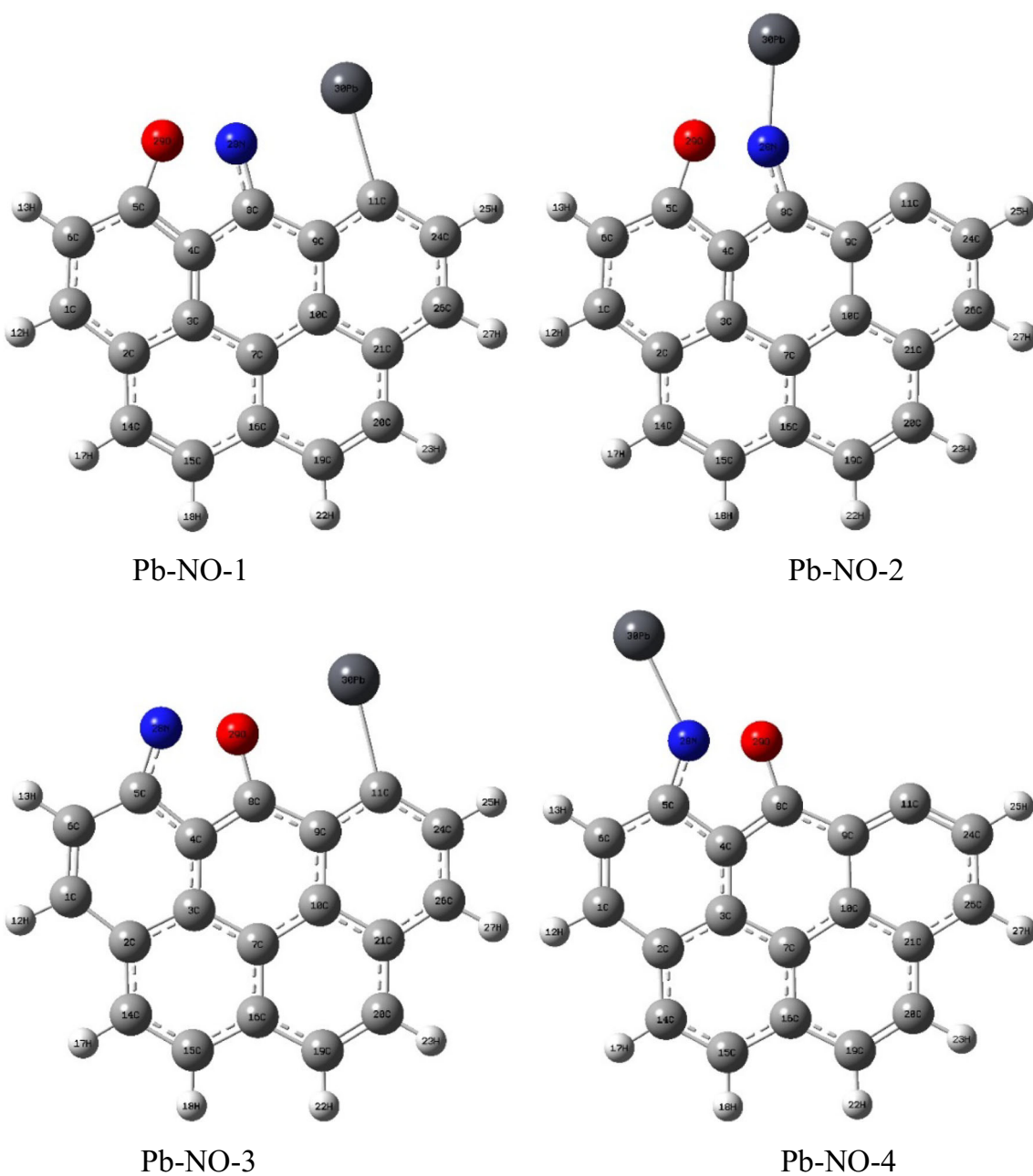

Pb-NO-1

Pb-NO-2

Pb-NO-3

Pb-NO-4

Fig. 8 Pb adsorption on NO-CS models

Table 7 Pb adsorption on NO-CS parameters

Model	Bond	Bond lengths(Å)	Bond population	Pb charge	E_{ads}(kJ mol^{-1})
Pb- NO-CS-1	C(11)-Pb(30)	2.284	0.273417	0.376272	−473.6
Pb- NO-CS-2	N(28)-Pb(30)	2.118	0.016609	0.293945	−181.7
Pb- NO-CS-3	C(11)-Pb(30)	2.265	0.27381	0.336652	−410.7
Pb- NO-CS-4	N(28)-Pb(30)	2.329	0.105606	0.277961	−167.3

The relationship between Pb charge and adsorption energy

Based on the above calculation results, data fitting between adsorption energy and Pb charge for three different carbonaceous surfaces adsorbed gas component was performed, as shown in Fig. 9. From Fig. 9, the linear relationship between Pb charge and adsorption energy can be clearly found. For carbonaceous surface adsorbed the same gas, the Pb charge is proportional to adsorption energy. In addition, the slope of linear fit of NO and CO is much more sharp than the linear of CO_2, indicating that the effect of Pb charge on elemental lead adsorption on carbonaceous surface adsorbed diatomic gas is much more significant than carbonaceous surface adsorbed triatomic gas. Furthermore, atomic charge is of great significance for analyzing the process of elemental lead adsorption.

Conclusions

Elemental lead and three kinds of flue gas adsorptions on carbonaceous surfaces were studied at B3PW91/6-31G(d)/SDD level by calculating the bond lengths, bond population, Mulliken charge, and adsorption energy. By analyzing the
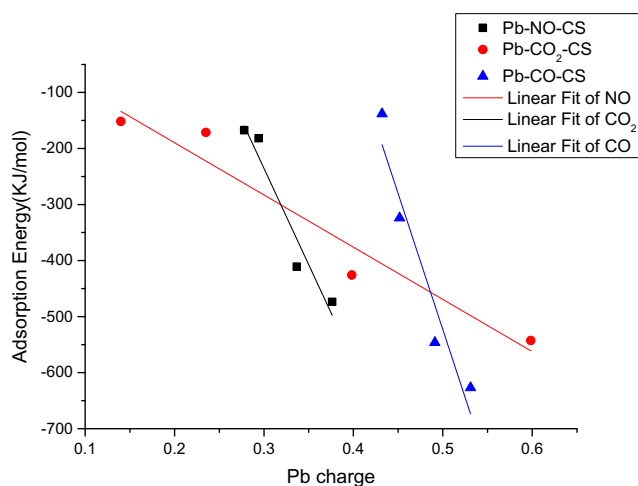
value of adsorption energy, we can conclude that all adsorption processes belong to chemical adsorption. Owing to multiple active sites on carbonaceous surface, there are many adsorption configurations for elemental lead, CO, CO_2, and NO. Moreover, the different adsorption sites have different adsorption energies, indicating that the adsorption process has significant affinity to adsorption sites.

Comparing the adsorption energy between elemental lead and three kinds of flue gas, the adsorptions energy of three kinds of flue gas are all larger than elemental lead on the carbonaceous surface, suggesting that CO, CO_2, and NO adsorptions on carbonaceous surfaces are more stable than elemental lead. Apart from those, it would seem logical to assume that there may be a competitive adsorption among the three kinds of flue gas and elemental lead. Furthermore, the adsorption strength order of three kinds of flue gas on the carbonaceous surfaces is $CO_2 > NO > CO > Pb$ on average.

Comparing the elemental lead adsorption energy between carbonaceous surfaces and carbonaceous surfaces adsorbed flue gases, we can conclude that elemental lead are more likely to adsorb on carbonaceous surfaces which adsorbed flue gases. Furthermore, analyzing the adsorption configurations and adsorption energy at different adsorption sites for the same flue gas, it is quite plausible that the adsorbed flue gases can increase the activity of its neighboring site which in turn increases the adsorption capacity of the carbonaceous surface for elemental lead. In addition, the enhancement order of three kinds of flue gas for elemental lead adsorption on carbonaceous surface is CO-CS > CO_2-CS > NO-CS > CS on average.

All in all, CO, CO_2, and NO can promote elemental lead adsorption on carbonaceous surfaces, but probably compete adsorption sites on carbonaceous surfaces with elemental lead. The present theoretical investigation could lay the foundation for the further study about the effect of carbon based injection on Pb removal. The good linear relationship between the atomic charge and the adsorption energy shows that the atomic charge is very helpful for analyzing elemental lead adsorption on carbonaceous surfaces. Further investigations will be carried out to study the effect of other flue gases on elemental lead adsorption on carbonaceous surfaces so as to complete the mechanism research.

Fig. 9 The relationship between adsorption energy and Pb charge

References

1. Iyer S, Sengupta C, Velumani A (2015) Lead toxicity: an overview of prevalence in Indians. Clinica Chimica Acta
2. Debelius B, Forja JM, DelValls Á et al. (2009) Toxicity and bioaccumulation of copper and lead in five marine microalgae. Ecotoxicol Environ Saf 72(5):1503–1513
3. Lee YH, Lee DH, Kim JH et al (1995) Blood lead levels in children. Korean J Occup Environ Med 7(1):82–87
4. Hildebrand MP (2011) Lead toxicity in a newborn. J Pediatr Health Care 25(5):328–331
5. Shen ZG, Li XD, Chen HM et al (2002) Phytoextraction of Pb from a contaminated soil using high biomass species of plants. J Environ Qual 31:1893–1900
6. Nriagu JO (1989) A global assessment of natural sources of atmospheric trace metals. Nature 338(6210):47–49
7. Li XL, Zhang YX, Tan MG et al (2009) Atmospheric lead pollution in fine particulate matter in Shanghai, China. J Environ Sci 21(8): 1118–1124
8. Tan MG, Zhang GL, Li XL et al (2006) Comprehensive study of lead pollution in Shanghai by multiple techniques. Anal Chem 78(23):8044–8050
9. Lou MT, Qin JF, Li ZX et al (2012) Review on lead pollution in China. Guangdong Trace Elem Sci 19(10):10–20
10. Qin JF, Li ZX, Lou MT et al (2010) Status sources of pollution and control measures of Chinese children lead poisoning. Guangdong Trace Elem Sci 17(1):1–13
11. Deng S, Zhang F, Liu Y et al (2013) Lead emission and speciation of coal-fired power plants in China. China Environ Sci 33(7): 1199–1206
12. Chen SJ, Xue JM, Xu YY et al (2015) Analysis on reduction of trace elements in flue gas by dust removing facilities in coal-fired power plants. Proc CSEE 35(9):2224–2230
13. Li J, Maroto-Valer MM (2012) Computational and experimental studies of mercury adsorption on unburned carbon present in fly ash. Carbon 50(5):1913–1924
14. Padak B, Brunetti M, Lewis A et al (2006) Mercury binding on carbonaceous. Environ Prog 25(4):319–326
15. Matsumura Y (1974) Adsorption of mercury vapor on the surface of activated carbons modified by oxidation or iodization. Atmos Environ (1967) 8(12):1321–1327
16. Hu C, Zhou J, He S et al (2009) Effect of chemical activation of an activated carbon using zinc chloride on elemental mercury adsorption. Fuel Process Technol 90(6):812–817
17. Zhang Y, Zhao L, Guo R et al (2015) Mercury adsorption characteristics of HBr-modified fly ash in an entrained-flow reactor. J Environ Sci 33:156–162
18. Mei Z, Shen Z, Zhao Q et al (2008) Removal and recovery of gasphase element mercury by metal oxide-loaded activated carbon. J Hazard Mater 152(2):721–729
19. Zhou Q, Duan YF, Hong YG et al (2015) Experimental and kinetic studies of gas-phase mercury adsorption by raw and bromine modified activated carbon. Fuel Process Technol 134:325–332
20. Padak B, Wilcox J (2009) Understanding mercury binding on activated carbon. Carbon 47(12):2855–2864
21. Montoya A, Truong TTT, Mondragon F et al (2001) CO desorption from oxygen species on carbonaceous surface: 1. Effects of the local structure of the active site and the surface coverage. J Phys Chem A 105(27):6757–6764
22. Montoya A, Mondragon F, Truong TN (2002) First-principles kinetics of CO desorption from oxygen species on carbonaceous surface. J Phys Chem A 106(16):4236–4239
23. Wu X, Radovic LR (2004) Ab initio molecular orbital study on the electronic structures and reactivity of boron-substituted carbon. J Phys Chem A 108(42):9180–9187
24. Radovic LR (2005) The mechanism of CO 2 chemisorption on zigzag carbon active sites: a computational chemistry study. Carbon 43(5):907–915
25. Chen N, Yang RT (1998) Ab initio molecular orbital study of the unified mechanism and pathways for gas-carbon reactions. J Phys Chem A 102(31):6348–6356
26. Chen N, Yang RT (1998) Ab initio molecular orbital calculation on graphite: Selection of molecular system and model chemistry. Carbon 36(7):1061–1070
27. Liu J, Cheney MA, Wu F et al (2011) Effects of chemical functional groups on elemental mercury adsorption on carbonaceous surfaces. J Hazard Mater 186(1):108–113
28. Liu J, Qu W, Yuan J et al (2009) Theoretical studies of properties and reactions involving mercury species present in combustion flue gases. Energy Fuel 24(1):117–122
29. Liu J, Qu W, Joo SW et al (2012) Effect of SO2 on mercury binding on carbonaceous surfaces. Chem Eng J 184:163–167
30. Frisch MJ, Trucks GW, Schlegel HB, Scuseria GE, Robb MA, Cheeseman JR et al (2010) Gaussian09, revision B.01. Gaussian Inc, Wallingford
31. Xin G, Zhao P, Zheng C (2009) Theoretical study of different speciation of mercury adsorption on CaO (001) surface. Proc Combust Inst 32(2):2693–2699